

**Combustion Air Humidification for NO<sub>x</sub> Emissions Reduction in Gas Boiler  
An Experimental Study**

Zhang, Qunli; Zhao, Wenqiang; Sun, Donghan; Meng, Xiangzhao; Hooman, Kamel; Yang, Xiaohu

**DOI**

[10.1080/01457632.2023.2171814](https://doi.org/10.1080/01457632.2023.2171814)

**Publication date**

2023

**Document Version**

Final published version

**Published in**

Heat Transfer Engineering

**Citation (APA)**

Zhang, Q., Zhao, W., Sun, D., Meng, X., Hooman, K., & Yang, X. (2023). Combustion Air Humidification for NO<sub>x</sub> Emissions Reduction in Gas Boiler: An Experimental Study. *Heat Transfer Engineering*, 45(1), 55-68. <https://doi.org/10.1080/01457632.2023.2171814>

**Important note**

To cite this publication, please use the final published version (if applicable).  
Please check the document version above.

**Copyright**

Other than for strictly personal use, it is not permitted to download, forward or distribute the text or part of it, without the consent of the author(s) and/or copyright holder(s), unless the work is under an open content license such as Creative Commons.

**Takedown policy**

Please contact us and provide details if you believe this document breaches copyrights.  
We will remove access to the work immediately and investigate your claim.

***Green Open Access added to TU Delft Institutional Repository***

***'You share, we take care!' - Taverne project***

**<https://www.openaccess.nl/en/you-share-we-take-care>**

Otherwise as indicated in the copyright section: the publisher is the copyright holder of this work and the author uses the Dutch legislation to make this work public.



## Combustion Air Humidification for NO<sub>x</sub> Emissions Reduction in Gas Boiler: An Experimental Study

Qunli Zhang, Wenqiang Zhao, Donghan Sun, Xiangzhao Meng, Kamel Hooman & Xiaohu Yang

To cite this article: Qunli Zhang, Wenqiang Zhao, Donghan Sun, Xiangzhao Meng, Kamel Hooman & Xiaohu Yang (2023): Combustion Air Humidification for NO<sub>x</sub> Emissions Reduction in Gas Boiler: An Experimental Study, Heat Transfer Engineering, DOI: [10.1080/01457632.2023.2171814](https://doi.org/10.1080/01457632.2023.2171814)

To link to this article: <https://doi.org/10.1080/01457632.2023.2171814>



Published online: 01 Feb 2023.



Submit your article to this journal [↗](#)



Article views: 7




View related articles [↗](#)



View Crossmark data [↗](#)



# Combustion Air Humidification for NO<sub>x</sub> Emissions Reduction in Gas Boiler: An Experimental Study

Qunli Zhang<sup>a,b</sup>, Wenqiang Zhao<sup>a,b</sup>, Donghan Sun<sup>a,b</sup>, Xiangzhao Meng<sup>c</sup>, Kamel Hooman<sup>d</sup>, and Xiaohu Yang<sup>c</sup> 

<sup>a</sup>Beijing Key Lab of Heating, Gas Supply, Ventilating and Air Conditioning Engineering, Beijing University of Civil Engineering and Architecture, Beijing, P.R. China; <sup>b</sup>Collaborative Innovation Center of Energy Conservation & Emission Reduction and Sustainable Urban-Rural Development in Beijing, Beijing, P.R. China; <sup>c</sup>Institute of Building Environment & Sustainability Technology, School of Human Settlements and Civil Engineering, Xi'an Jiaotong University, Xi'an, P.R. China; <sup>d</sup>Process & Energy Department, Delft University of Technology, Delft, The Netherlands

## ABSTRACT

NO<sub>x</sub> emission reduction from gas boilers has become a key issue in improving air quality. Combustion air humidification technology is gradually being used to reduce NO<sub>x</sub> emissions. However, the NO<sub>x</sub> emission reduction effect of gas boilers at a higher combustion air humidity has been studied less. A flue gas with low NO<sub>x</sub> emissions and a waste heat recovery system using combustion air humidification technology are proposed in this study. In the ultra-low NO<sub>x</sub> mode, the effect of high combustion air humidity on NO<sub>x</sub> emission reduction and efficiency of the gas boiler were studied experimentally. In the waste heat recovery mode, the effects of the heat network backwater temperature on the NO<sub>x</sub> emission reduction and system efficiency were studied experimentally. Results showed that an increase in air humidity can significantly reduce the NO<sub>x</sub> concentration formed by combustion. The ultra-low NO<sub>x</sub> mode reduces NO<sub>x</sub> emissions from 130 mg/m<sup>3</sup> to 23.3 mg/m<sup>3</sup> and affects the boiler efficiency slightly. In the waste heat recovery mode, NO<sub>x</sub> emissions can be reduced to 39.9 mg/m<sup>3</sup> when the backwater temperature of the heat network is 55 °C. This condition improves the efficiency to 93.8%. The analysis results provide suggestions for the selection of the operation modes.

## Introduction

The thermal efficiency of gas-fired heating boilers is higher than that of coal-fired boilers. Compared to coal, natural gas is regarded as a cleaner energy source with less carbon emissions and air contamination in the combustion process [1]. Gas boiler combustion produces nitrogen oxides (NO<sub>x</sub>), which generate fog and haze [2]. NO<sub>x</sub>, which has a significant impact on the atmosphere, mainly refers to a variety of nitrogen and oxygen compounds, namely NO, NO<sub>2</sub>, N<sub>2</sub>O, N<sub>2</sub>O<sub>3</sub>, N<sub>2</sub>O<sub>4</sub>, and N<sub>2</sub>O<sub>5</sub> [3]. Acidifying substance emissions damage human health, ecosystems, buildings, and materials [4]. Boilers that heat buildings emit large amounts of NO<sub>x</sub>. Thus, improving air quality and developing clean heating are of great significance. Cities, such as Beijing, Tianjin, and Zhengzhou, have introduced strict local standards. However, majority of the existing boilers exceed these standards

and cannot be used. Therefore, nitrogen oxide emission reduction technology for gas boilers has become a hot issue in the industry.

Generally, an increase in furnace temperature promotes NO<sub>x</sub> production. Recently, humidification combustion technology has been used to reduce NO<sub>x</sub> production because of its ability to lower the combustion temperatures. This technology was first used for engines and gas turbines. Wu et al. [5] investigated the effect of water-spraying technology on the combustion and emission characteristics of heavy natural gas engines through numerical simulations. According to the simulation results, an increase in spray mass decreases the flame propagation speed, reduces the rate of fuel heat release, extends the duration of combustion, and decreases the maximum temperature. This behavior significantly reduces the thermal engine load and inhibits NO<sub>x</sub> production. Jonsson and Yan [6] summarized the study of humidified gas turbine

## Nomenclature

$a$	estimated standard deviation of the mean distribution	$T_a$	combustion air temperature ( $^{\circ}\text{C}$ )
BEVP	boiler equipped with a vapor pump	$T_b$	backwater temperature of the heat network, ( $^{\circ}\text{C}$ )
$B$	natural gas consumption ( $\text{Nm}^3/\text{h}$ )	$T_H$	supply water temperature of the heat network ( $^{\circ}\text{C}$ )
CNY	Chinese Yuan	$T_{FI}$	flue gas temperature of boiler ( $^{\circ}\text{C}$ )
$C_m$	mass concentration ( $\text{mg}/\text{m}^3$ )	$T_s$	spray temperature of exchanger B ( $^{\circ}\text{C}$ )
$C_m, \text{NO}_x$	$\text{NO}_x$ mass concentration	$T_w$	backwater temperature of the heat network after preheating ( $^{\circ}\text{C}$ )
CN	hydrocyanic acid root	ULN	ultra-low $\text{NO}_x$ emission
$c_p$	constant pressure specific heat of water ( $\text{kJ}/(\text{kg}\cdot\text{K})$ )	$u_1$	uncertainty caused by repeated measurement of NO
$C_{PPM, \text{NO}}$	PPM concentrations of NO	$u_2$	uncertainty caused by repeated measurement of $\text{NO}_2$
$C_{PPM, \text{NO}_2}$	PPM concentrations of $\text{NO}_2$	$u_3$	uncertainty caused by an error in the flue gas analyzer
CO	carbon monoxide	$u_c$	combined standard uncertainty
FGLNHR-CAH	flue gas low $\text{NO}_x$ emission and waste heat recovery system using combustion air humidification technology	$u_i$	a component of uncertainty
$F_s$	spray flow ( $\text{m}^3/\text{h}$ )	$u_{xi}$	measurement standard uncertainty
$\partial f/\partial x_i$	the transfer coefficient of the effect of $u_{xi}$ on the measured estimate	$\nu$	degrees of freedom
$H_a$	combustion air humidity ( $\text{g}/\text{kg}$ Dry air)	$V_m$	molar volume of gas
HCN	hydrogen cyanide	WHR	waste heat recovery
LGR	liquid gas ratio of exchanger B	$x$	arithmetic mean value
$m$	mass flowrate of heat network ( $\text{kg}/\text{s}$ )	$x_i$	measured value
$M_{\text{NO}_2}$	relative molecular mass of $\text{NO}_2$		
$n$	number of measurements		
$N$	nitrogen atoms	<b>Greek symbols</b>	
NO	nitric oxide	$\varphi$	uncertainty
$\text{NO}_2$	nitrogen dioxide	$\sigma$	estimated value of the standard deviation of a single measurement
$\text{NO}_x$	nitrogen oxide	$\sigma_u/u$	relative standard deviation of $u$
$N_2$	nitrogen	$\eta_{\text{Boiler}}$	boiler efficiency
$N_2\text{O}$	nitrous oxide	$\eta_{\text{Total}}$	total system efficiency
$N_2\text{O}_3$	dinitrogen trioxide		
$N_2\text{O}_4$	dinitrogen tetroxide		
$N_2\text{O}_5$	nitrogen pentoxide		
O	oxygen atom	<b>Subscripts</b>	
$\text{O}_2$	oxygen	$a$	combustion air
OH	hydroxide ion	$b$	backwater
$Q_{out}$	output heat of gas boiler ( $\text{kJ}/\text{Nm}^3$ )	$in$	input
$Q_{in}$	input heat of gas boiler ( $\text{kJ}/\text{Nm}^3$ )	$out$	output
$Q_{net,ar}$	low calorific value of natural gas ( $\text{kJ}/\text{Nm}^3$ )	$s$	spray water
$Q_w$	waste heat recovery quantity ( $\text{kJ}/\text{Nm}^3$ )		

combustion and proposed that humidification reduces the generation of NO in the combustion process.

As humidification technology has been proven to achieve  $\text{NO}_x$  reduction in engines and gas turbines, researchers have applied humidification technology to gas boilers. However, humidification combustion reduces boiler efficiency [7]; therefore, thermal efficiency should be considered. Waste heat recovery (WHR) can improve the energy utilization rate and reduce energy waste [8–12]. Compared to other fuels, natural gas combustion produces more water vapor. Hence, there is more latent heat in the flue gas to recover [13, 14]. Therefore, researchers have mostly used WHR technology to improve thermal efficiency when utilizing humidification technology.

Lee et al. [15] used condensed water to humidify air. When the air temperature was low, the moisture

content in the saturated state was low. The system uses condensate water to humidify the furnace directly so that the system can achieve higher moisture content conditions. Generally, boiler efficiency under spray technology has been studied, and no specific study on  $\text{NO}_x$  has been conducted. Wang et al. [16] proposed a boiler equipped with a vapor pump (BEVP) system, which humidifies the combustion air. Although the heat transfer characteristics of the BEVP system have been studied,  $\text{NO}_x$  emission reduction has not been studied. Chen et al. [7, 17] proposed a new non-contact total heat exchanger to supply air and flue gas for heat recovery. Additionally, they studied the influence of air humidification on the efficiency and emissions of the boiler. The research findings showed that air humidification improved the overall boiler efficiency and reduced  $\text{NO}_x$  concentration.

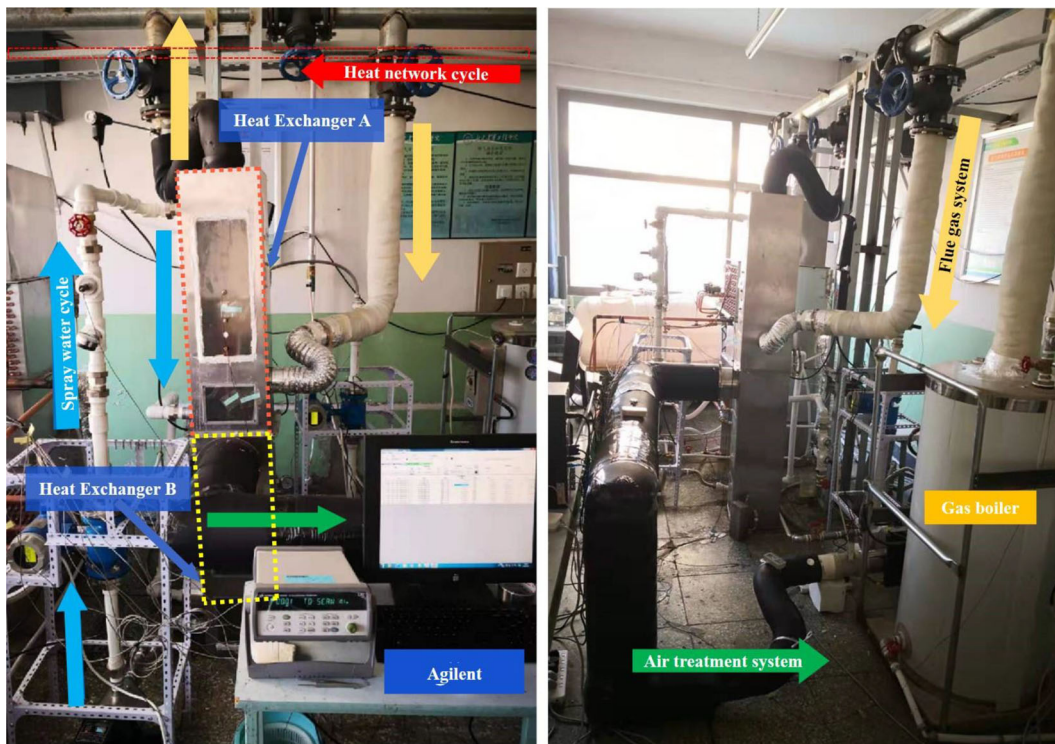


Figure 1. FGLNHR-CAH system experiment bench.

However, the maximum air humidity in their study was  $48 \text{ g/kg}_{\text{Dry air}}$  and higher air humidity conditions were not considered. Zhang et al. [18] proposed an exhaust gas condensation heat recovery system that synergized with a low nitrogen oxide discharge system. However, the factors influencing  $\text{NO}_x$  emission reduction were not explained. Men et al. [19] proposed a new flue gas WHR system equipped with an enthalpy wheel, which was used to recover the waste heat and water of the flue gas. They studied the effect of system air humidification but did not study the effect of  $\text{NO}_x$  emission reduction.

In the aforementioned studies, the  $\text{NO}_x$  reduction effect of gas boilers at higher combustion air humidity has not been studied extensively. Moreover, majority of systems use flue gas waste heat to heat humidified combustion air, and there is competition between the waste heat used to heat the air and the recycled waste heat, which affects the  $\text{NO}_x$  emission reduction of the system. However, the effect of flue gas WHR on  $\text{NO}_x$  emission reduction has not yet been studied in detail.

A flue gas with low  $\text{NO}_x$  emissions and a WHR system using combustion air humidification technology were proposed (FGLNHR-CAH). Additionally, ultra-low  $\text{NO}_x$  (ULN) emission and WHR modes were proposed. The efficiency and  $\text{NO}_x$  emission reduction effects of gas boilers under high air humidity were also investigated. Subsequently, the effect of WHR on the  $\text{NO}_x$  reduction effect and system efficiency was

studied, and the mechanism of  $\text{NO}_x$  emission reduction by air humidification and the economic applicability of different operation modes were discussed.

## Experimental

### System description

The experimental system of FGLNHR-CAH was composed of a gas boiler, water tank, direct contact heat exchangers A and B, plate heat exchanger, and water pump, as shown in Fig. 1. Heat exchanger B was the core equipment used for heating and humidifying the combustion air. The specific parameters of the experimental flue gas, which was obtained from a 58 kW vertical gas boiler, are listed in Table 1.

The operating mode of the system could be adjusted using a valve. In the ULN mode, valves b and c are closed, and valves a and d are opened. In the WHR mode, valves a and d are closed, and valves b and c are opened. The system flow chart is shown in Figs. 2 and 3. The experimental system consisted of four parts: the flue gas system, air treatment system, spray water cycle, and heat network cycle.

ULN mode:

1. Flue gas system: The flue gas system consisted mainly of a gas boiler and a direct contact heat exchanger. The high-temperature flue gas was



discharged from the boiler and through the pipeline into heat exchanger A, which was a spray-type heat exchanger with flue gas and sprayed water to exchange heat and mass. The flue gas was passed through a screen mist remover to remove moisture, which discharged into the atmosphere.

2. Air treatment system: Direct contact heat exchanger B was the core equipment. The water in the water storage tray of heat exchanger A directly enters heat exchanger B as spray water heating and humidifying combustion air. To prevent excess water from entering the burner, a screen defogging device was set at the exit of heat exchanger B.
3. Spray water cycle: Spray water is the main medium for heat transfer in the system. The low-temperature spray water and high-temperature flue gas achieved a complete heat exchange in heat exchanger A. After the low-temperature spray water was heated, the water pump was fed into heat exchanger B to exchange heat and mass with the combustion air. Finally, the spray water in heat exchanger B was returned to heat exchanger A.

4. Heat network cycle: The hot water in the boiler was supplied to the thermal user and returned to the boiler for further heating.

WHR mode:

The flow of the flue gas and air treatment systems was the same as that in the ULN mode.

1. Spray-water cycle: After being heated by the flue gas in heat exchanger A, the spray water first enters the plate heat exchanger to heat the heat network return water. Then, it enters heat exchanger B to humidify the combustion air. Finally, it returns to heat exchanger A to exchange heat with the flue gas.
2. Heat network cycle: Hot water in the boiler was supplied to the thermal user. The heat network backwater entered the plate heat exchanger first and then returned to the boiler for further heating.

Additional operating parameters of this system are listed in Table 2.

**Table 1.** Boiler operating parameters.

Parameters	Unit	Value
Boiler heat capacity	kW	58
Natural gas consumption	Nm <sup>3</sup> /h	5.7
Excess air ratio	—	1.2
Boiler load	%	90
Flue gas temperature	°C	205.8
Flow rate of boiler water supply	L/min	31
Original boiler efficiency	%	87.5

### Test methods

The distribution of the measurement points in this experimental platform is shown in Fig. 2, and the test equipment is listed in Table 3. The main test instruments included an electromagnetic flowmeter, flue gas analyzer, temperature and humidity recording instrument, electromagnetic flowmeter, and thermocouple. An Agilent data-acquisition module was used as the

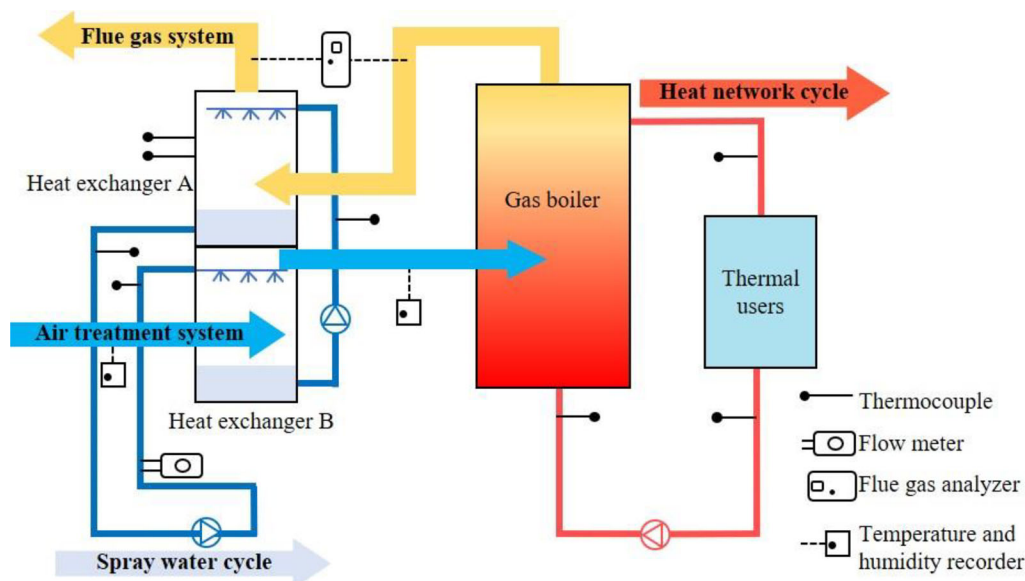


**Figure 2.** Flow chart of ULN mode of FGLNHR-CAH system.

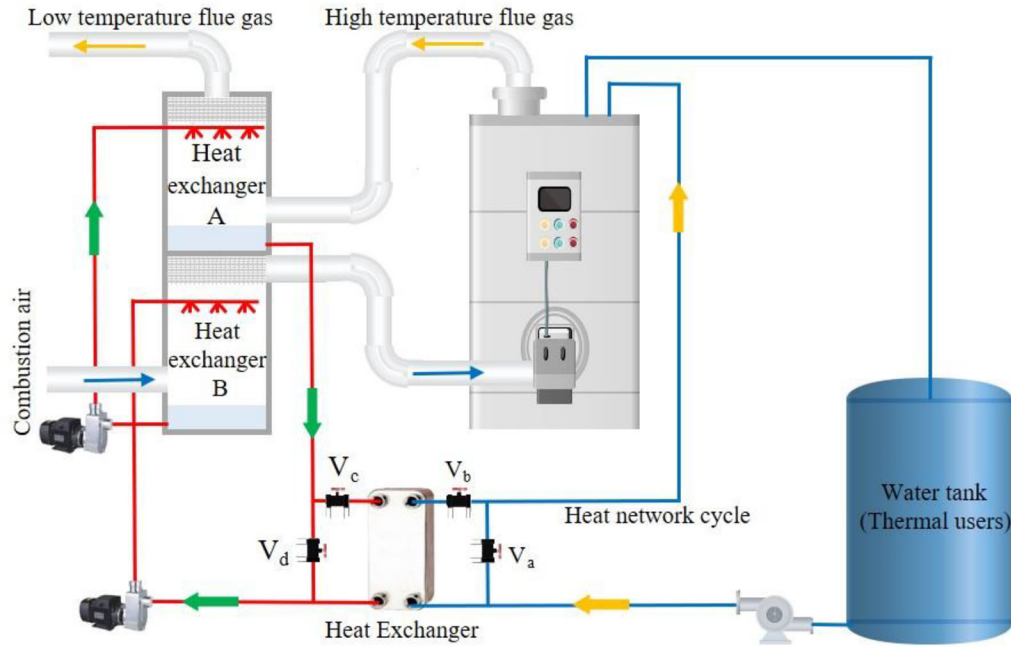


Figure 3. Flow chart of WHR mode of FGLNHR-CAH system.

Table 2. Operating parameters of the FGLNHR-CAH system.

System	Mode	$T_s$	$T_b$	$F_s$						
		°C	°C	m <sup>3</sup> /h						
FGLNHR-CAH	ULN mode	59.6	—	0.21	0.35	0.43	0.54	0.65	0.74	0.84
	WHR mode 1	54.7	55	0.23	0.34	0.41	0.52	0.63	0.74	0.82
	WHR mode 2	49.9	50	0.24	0.36	0.43	0.54	0.63	0.74	0.82
	WHR mode 3	45.8	45	0.25	0.35	0.43	0.54	0.64	0.73	0.83

Table 3. Details of the test equipment.

Parameter	Equipment	Model	Accuracy
Flue gas temperature	Flue gas analyzer	Testo340	±0.5%(reading)
NO concentration	Flue gas analyzer	Testo340	±5 ppm (0-99 ppm)
NO <sub>2</sub> concentration	Flue gas analyzer	Testo340	±10 ppm (0-199 ppm)
Water temperature	Thermocouple	T-type thermocouple	±0.3 °C
Spray water flow	Electromagnetic Flowmeter	LDYD3-032-16-1-1	±0.5%(reading)
Air temperature	Temperature and humidity recorder	WWSZY-1	±0.3 °C(-50-100 °C)
Air humidity ratio	Temperature and humidity recorder	WWSZY-1	±2%RH (reading)
Air velocity	Digital Anemometer	AS8336	±0.03 m/s (0.3-45 m/s)

experimental platform. Data was recorded every 5 s when the system was running stably. In total, 240 sets of data were measured for each condition.

### Uncertainty analysis

According to the methods described in error theory and data processing [20], the primary sources of uncertainty when measuring the NO<sub>x</sub> concentration were analyzed, and the standard uncertainty that resulted from all types of elements was tested using a detailed direct evaluation method.

In case of uncertainties, errors exist between the test data and truth value. Herein, the uncertainty propagation of the measurement and experimental data are analyzed theoretically. Hence, the direct error analysis method was calculated using:

$$\varphi = \frac{\sqrt{\sum_{i=1}^n (x_i - \bar{x})^2}}{n(n-1)} \quad (1)$$

where  $\varphi$  refers to the uncertainty,  $n$  is the number of data tests, and  $x_i$  is the data value of the  $i^{\text{th}}$  measurement.  $\bar{x}$  denotes the arithmetic average of the experimental data in each group in the form of:



**Table 4.** Uncertainty calculation equation [20].

Purpose	Uncertainty equation
Standard deviation	$\sigma = \sqrt{\frac{\sum_{i=1}^n (x_i - \bar{x})^2}{n-1}}$ (3)
Measurement standard uncertainty The assessment method of class A (n times)	$u_{x_i} = \sigma_i / \sqrt{n}$ (4)
Measurement standard uncertainty The assessment method of class B (uniform distribution)	$u_{x_i} = a / \sqrt{3}$ (5)
Degrees of freedom (The assessment method of class A)	$v = n - 1$ (6)
Degrees of freedom (The assessment method of class B)	$v = \frac{1}{2 \left( \frac{\sigma_u}{u} \right)^2}$ (7)
A component of uncertainty	$u_i = \left  \frac{\partial f}{\partial x_i} \right  u_{x_i}$ (8)
Combined standard uncertainty	$u_c = \sqrt{\sum_{i=1}^n u_i^2}$ (9)

$$\bar{x} = \sum_{i=1}^n x_i / n \quad (2)$$

Using the same method, an uncertainty analysis was performed for all operating conditions. The main calculation equations are listed in Table 4, see equations (3) - (9). To avoid random error, all the measurements were repeated 5 times with equal accuracy to determine the error margin.

The mass concentration of NO<sub>x</sub> was calculated according to NO<sub>2</sub>, and the equation is as follows:

$$C_{m,NO_x} = \frac{M_{NO_2}(C_{PPM,NO} + C_{PPM,NO_2})}{V_m} \quad (10)$$

The calculation considers H<sub>a</sub> = 49 g/kg<sub>dry air</sub> in WHR mode 1 as an example. The calculated arithmetic mean was 22.36 ppm for NO and 4.87 ppm for NO<sub>2</sub>. The estimated amount of NO<sub>x</sub> according to equation (10) was 55.91 mg/m<sup>3</sup>.

The main factors that had a significant influence on the NO<sub>x</sub> measurement uncertainty were as follows: uncertainties u<sub>1</sub> and u<sub>2</sub> were caused by the measurement repeatability of NO and NO<sub>2</sub>, respectively, and uncertainty u<sub>3</sub> was caused by an error in the flue gas analyzer. According to an analysis of these uncertainty characteristics, the assessment method of class A was used for uncertainties u<sub>1</sub> and u<sub>2</sub>, whereas that of class B was used for uncertainty u<sub>3</sub>.

By calculation, the standard uncertainty components that were caused by the measurement repeatability of NO and NO<sub>2</sub> were 0.61 mg/m<sup>3</sup> (239 degrees of freedom) and 0.17 mg/m<sup>3</sup> (239 degrees of freedom), respectively. The standard uncertainty component caused by the value error of the flue gas analyzer was 13.26 mg/m<sup>3</sup> according to Equations (5) and (8). The relative standard deviation was 10% and the corresponding degree of freedom was calculated to be 50 using Equation (7). Uncertainties u<sub>1</sub>, u<sub>2</sub>, and u<sub>3</sub> were

independent, and the combined standard uncertainty was 13.28 mg/m<sup>3</sup>. The final measurement of NO<sub>x</sub> was 55.91 ± 13.28 mg/m<sup>3</sup>. The errors of the other parameters are similar to those in the abovementioned analysis.

### Performance evaluation index

The performance evaluation indicators were defined. The output heat of the gas boiler (Q<sub>out</sub>), input heat of the gas boiler (Q<sub>in</sub>), WHR quantity (Q<sub>w</sub>), boiler efficiency (η<sub>Boiler</sub>), and the total system efficiency (η<sub>Total</sub>) are expressed as follows:

$$Q_{out} = c_p m (T_H - T_b) \quad (11)$$

$$Q_{in} = B \cdot Q_{net,ar} \quad (12)$$

$$Q_w = c_p m (T_w - T_b) \quad (13)$$

$$\eta_{Boiler} = \frac{Q_{out}}{Q_{in}} \quad (14)$$

$$\eta_{Total} = \frac{Q_{out} + Q_w}{Q_{in}} \quad (15)$$

where c<sub>p</sub> is the constant pressure specific heat of water, kJ/(kg·K); m is the mass flow rate, kg/s; T<sub>H</sub> is the supply water temperature of the heat network, °C; T<sub>b</sub> is the backwater temperature of the heat network, °C; B is the natural gas consumption, Nm<sup>3</sup>/h; Q<sub>net,ar</sub> is the low calorific value of natural gas, kJ/Nm<sup>3</sup>; and T<sub>w</sub> is the backwater temperature of the heat network after preheating, °C.

### Results

In this section, we present the results of the combustion experiments. The influence of combustion air humidity on system performance (boiler efficiency, NO<sub>x</sub> emissions, NO<sub>x</sub> emission stability, etc.) was

studied. The effect of the WHR mode on the  $\text{NO}_x$  emissions and total system efficiency was also studied.

### Effect of combustion air humidity on gas boiler efficiency

Boiler efficiency is an important system evaluation index. Boiler efficiency can be calculated using Eq. (14). In the experiment, the temperature and humidity of the combustion air were increased simultaneously, and the boiler efficiency was affected by two factors. After numerous tests, the average efficiency of the experimental boiler without the FGLNHR-CAH system was 87.5%. After being added to the system, with the increase in combustion air humidity, the change in boiler efficiency did not show an obvious rule, but most of the test results were slightly lower than the original boiler efficiency, as shown in Fig. 4. The average efficiency of the system decreased by 0.7% with FGLNHR-CHA.

### Effect of combustion air humidity on $\text{NO}_x$ emissions

Combustion air with different humidity was directed into the burner to study the effect of air humidity on  $\text{NO}_x$  concentration in the flue gas. For comparison, the  $\text{NO}_x$  emission concentration of the boiler under non-humidification conditions was tested experimentally. Under this condition, the air humidity was  $3.2 \text{ g/kg}_{\text{Dry air}}$  and the  $\text{NO}_x$  concentration in the flue gas reached  $130 \text{ mg/m}^3$ .

The  $\text{NO}_x$  concentration of the system was reduced to  $58.7 \text{ mg/m}^3$  by humidifying air to  $38.9 \text{ g/kg}_{\text{Dry air}}$ . When the air humidity increased to  $101.2 \text{ g/kg}_{\text{Dry air}}$ , the  $\text{NO}_x$  in the flue gas was reduced to  $23.3 \text{ mg/m}^3$ .

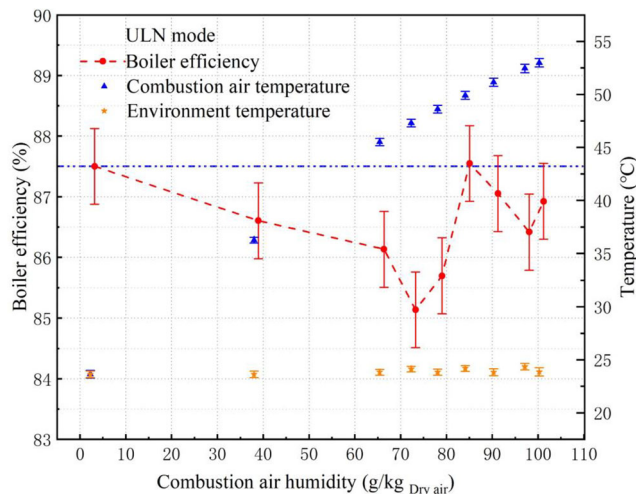


Figure 4. Effect of air humidity on boiler efficiency (ULN mode).

The  $\text{NO}_x$  emission reduction effect was better under high air humidity conditions. According to the experimental results, the  $\text{NO}_x$  concentration gradually decreased with an increase in air humidity, as shown in Fig. 5.

### Effect of combustion air humidity on $\text{NO}$ and $\text{NO}_2$ concentration

The  $\text{NO}_x$  in the gas boiler flue gas was composed mainly of  $\text{NO}$  and  $\text{NO}_2$ . The results show that the  $\text{NO}$  concentration in the flue gas decreases significantly with an increase in humidity in the combustion air, but the concentration of  $\text{NO}_2$  increases slightly, as shown in Fig. 6. According to the formation mechanism of  $\text{NO}_x$  (discussed in detail in the next section), the thermal  $\text{NO}_x$  formed by gas combustion was composed mainly of  $\text{NO}$ . Combustion air humidification technology reduced the generation of thermal  $\text{NO}_x$ ; thus, the  $\text{NO}$  production in the experiment decreased significantly. Through experiments and numerical simulations, Wang et al. [21] found that within a certain temperature range, a lower thermal combustion product temperature resulted in a higher likelihood of  $\text{NO}_2$  generation. Combustion air humidification technology can reduce the furnace temperature [22]; therefore, a decrease in temperature results in an increase in  $\text{NO}_2$  concentration in the flue gas.

### Effect of combustion air humidity on $\text{NO}_x$ emission stability test

When the system was running steadily,  $\text{NO}_x$  concentration was tested every 5 s, and the  $\text{NO}_x$  emissions is determined as shown in Uncertainty Analysis ( $55.91 \pm 13.28 \text{ mg/m}^3$ ). Each working condition was tested for at least 20 min.

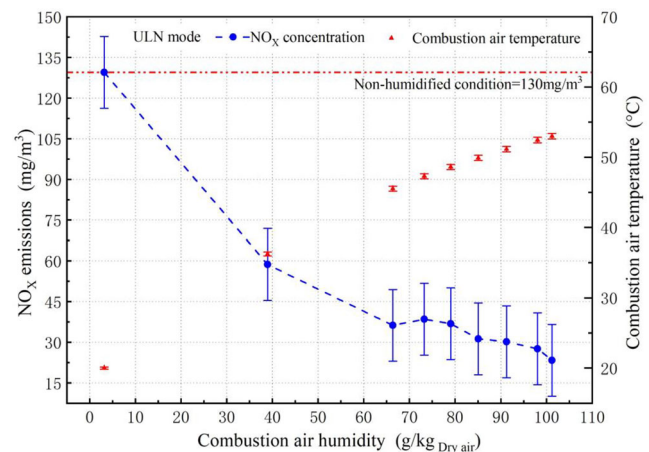


Figure 5. Effect of air humidity on  $\text{NO}_x$  emissions (ULN mode).

The  $\text{NO}_x$  emissions under different combustion air humidity conditions in WHR mode 1 are shown in Fig. 7. It can be seen that although the  $\text{NO}_x$  concentration fluctuates, the fluctuation range is small. The stability of  $\text{NO}_x$  emissions can be reflected intuitively. The standard deviations for the six working conditions were 0.424, 0.634, 0.940, 0.471, 0.478, and 0.496, respectively. These values are small and can reflect the stability of  $\text{NO}_x$  emissions.

### Effect of flue gas WHR on $\text{NO}_x$ emission

In this section, we describe the effect of WHR on the  $\text{NO}_x$  emission concentration in the system. The

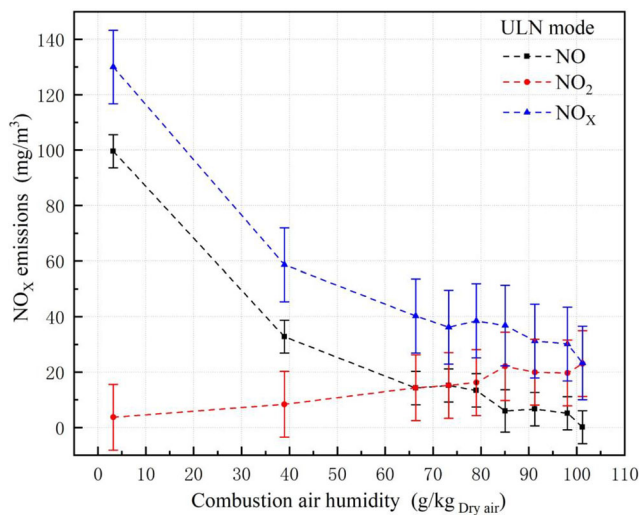


Figure 6. Effect of air humidity on NO and  $\text{NO}_2$  emissions (ULN mode).

temperature of the flue gas discharged by the system is shown in Fig. 8. The flue gas temperature of the original boiler was  $205.8^\circ\text{C}$ . The FGLNHR-CAH system can reduce the flue gas temperature to less than  $100^\circ\text{C}$  under all operating conditions. Additionally, with an increase in the spray water flow of heat exchanger A, the flue gas temperature decreased gradually. The flue gas temperature in WHR mode 3 is the lowest and can be reduced to  $51.5^\circ\text{C}$ .

For  $\text{NO}_x$  emission reduction, the most essential difference between the different operation modes is the spray water temperature in heat exchanger B, which directly affects the combustion air temperature. The liquid gas ratio (LGR) of heat exchanger B is the ratio of the mass flow rate of the spray water to the mass

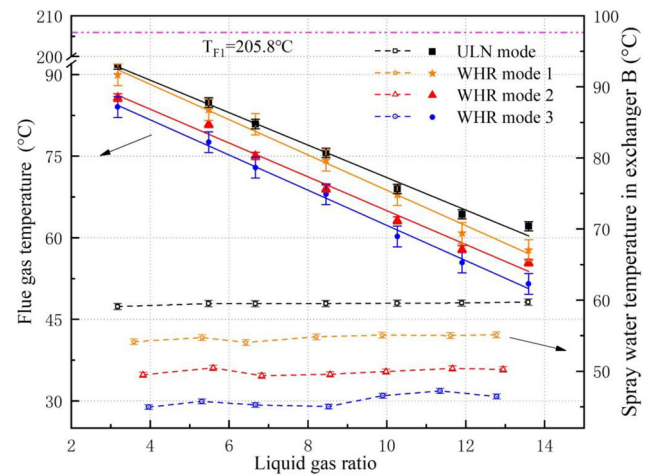


Figure 8. Effect of LGR on spray water temperature in exchanger B and flue gas temperature.

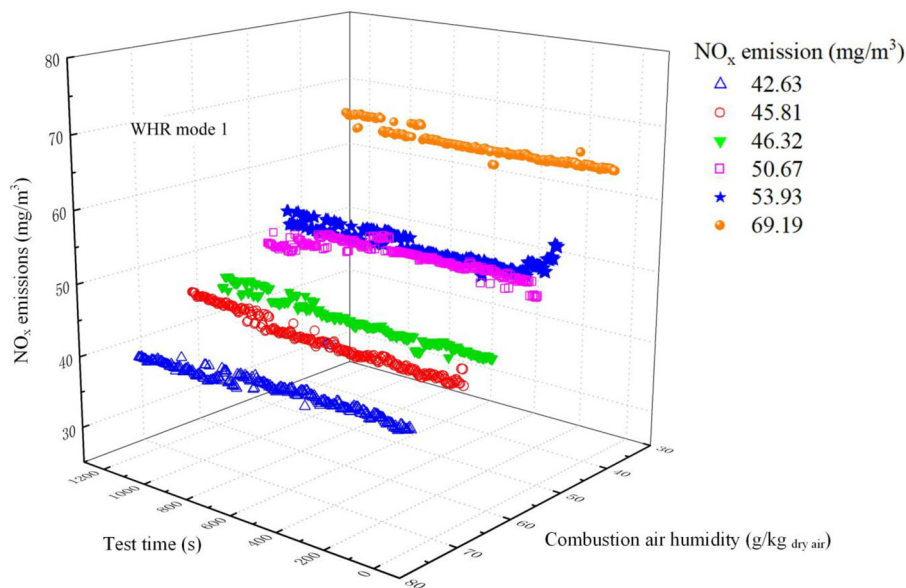


Figure 7.  $\text{NO}_x$  emission stability test for different air humidity in WHR mode 1.

flow rate of air. In the ULN mode, the average temperature of the spray water was  $59.6^{\circ}\text{C}$ . In the WHR mode, the backwater temperatures of the heat network were 45, 50, and  $55^{\circ}\text{C}$ . According to the system process, the backwater temperature of the heat network directly affected the spray temperature of heat exchanger B. The average temperatures recorded in the WHR mode were 54.7, 49.9, and  $45.8^{\circ}\text{C}$ , as shown in Fig. 8.

For a certain airflow rate, LGR was improved by increasing the spray flow rate. With an increase in LGR, the combustion air temperature increased nonlinearly. For the same LGR, a higher spray water temperature results in a higher combustion air temperature, as shown in Fig. 9. With an increase in

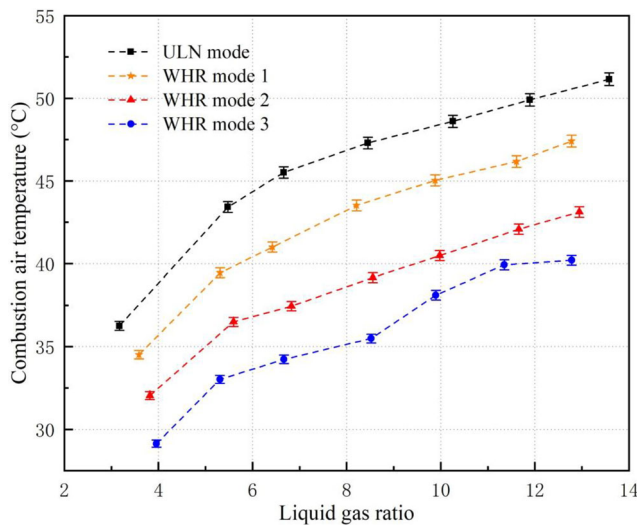


Figure 9. Effect of LGR on combustion air temperature.

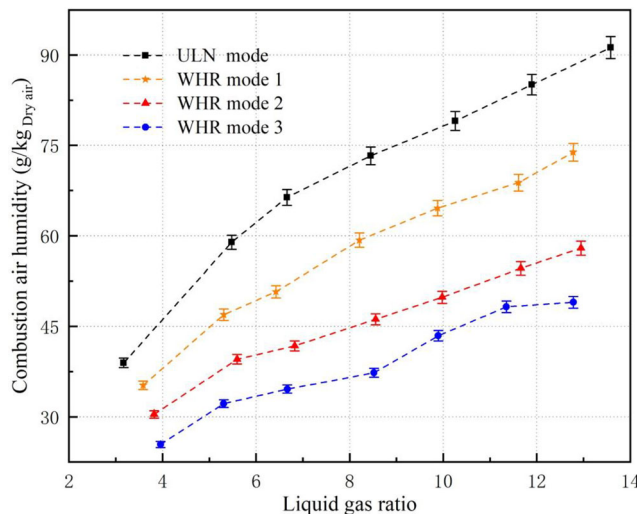


Figure 10. Effect of LGR on combustion air humidity.

LGR, the combustion air humidity increased nonlinearly, and the increasing trend slowed gradually, as shown in Fig. 10. The maximum combustion air humidity was different for different operation modes. The reason for this phenomenon is the effect of air temperature on saturation. Higher temperatures result in higher air saturation [23]. The ULN mode without WHR had the highest spray water temperature; therefore, the combustion air temperature and humidity were the highest for the same LGR. In the actual operation mode, the maximum combustion air humidity was  $101.2\text{ g/kg}_{\text{Dry air}}$ .

The  $\text{NO}_x$  emission concentration and total efficiency of the system in different operating modes were experimentally tested. Under different modes, the maximum combustion air humidity was different; therefore, the effect of  $\text{NO}_x$  emission reduction and total efficiency varied, as shown in Figs. 11 and 12.

In WHR mode 3, the maximum combustion air humidity was  $49\text{ g/kg}_{\text{Dry air}}$ ,  $\text{NO}_x$  emissions were  $50\text{ mg/m}^3$ , and total efficiency was 96.6%. In WHR mode 2, the maximum combustion air humidity was  $57.9\text{ g/kg}_{\text{Dry air}}$ ,  $\text{NO}_x$  emissions were  $46.4\text{ mg/m}^3$ , and total efficiency was 94.1%. In WHR mode 1, the maximum combustion air humidity was  $73.8\text{ g/kg}_{\text{Dry air}}$ ,  $\text{NO}_x$  emissions were  $39.9\text{ mg/m}^3$ , and the total efficiency was 93.8%. In the ULN mode, the maximum combustion air humidity was  $101.2\text{ g/kg}_{\text{Dry air}}$ ,  $\text{NO}_x$  emissions were  $23.3\text{ mg/m}^3$ , and the total efficiency was 86.9%.

Therefore, the  $\text{NO}_x$  emission reduction effect of the ULN mode is the best, but it affects boiler efficiency. The WHR mode can also reduce  $\text{NO}_x$  emissions, and the emission reduction effect is not as good as that of the ULN mode. However, the system efficiency improved through WHR.

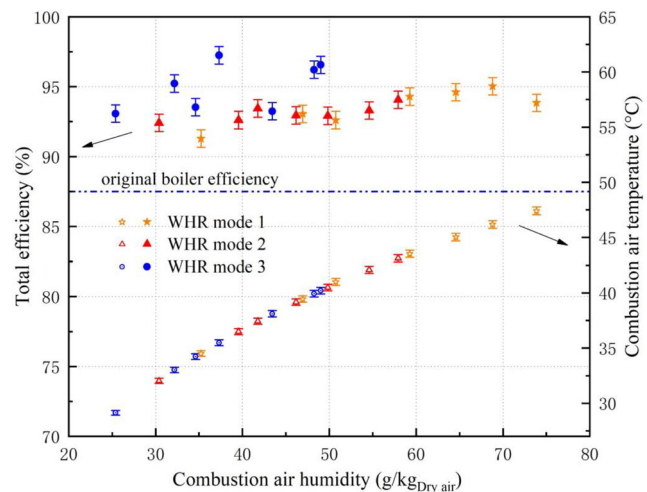


Figure 11. Effect of air humidity on the total efficiency.



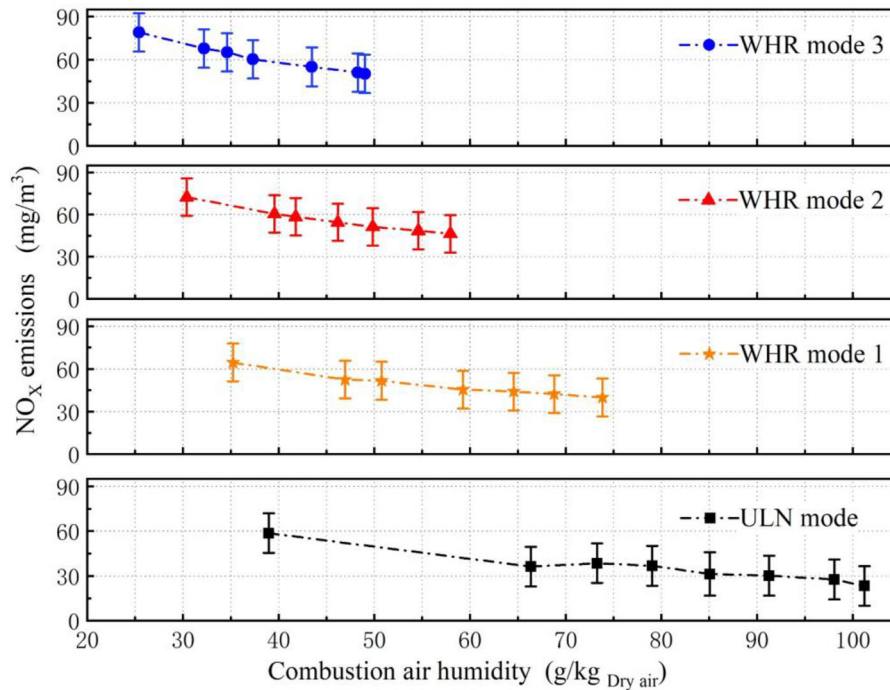


Figure 12. Effect of air humidity on NO<sub>x</sub> emissions.

## Discussion

### *NO<sub>x</sub> emission reduction mechanism of combustion air humidification technology*

The formation mechanism of nitrogen oxides includes three types: thermal, fast, and fuel. The thermal nitrogen oxides mechanism as put forward by Yakov Borisovich Zel'dovich (1914 – 1987) [24] explains an atomic chain mechanism for nitrogen oxide formation at high temperature, i.e., 1500 °C through chemical reactions, as shown in Fig. 13. According to Fenimore [25], prompt-NO<sub>x</sub> is the most important mechanism. Prompt-NO is generated by the reaction of nitrogen with hydrocarbon radicals and O<sub>2</sub>. Skreiberg et al. [26] proposed that prompt-NO in a majority of combustion systems accounts for less than 5% of all NO. Lupianez et al. [27] demonstrated that Fuel-NO<sub>x</sub> is formed by nitrogen oxides inherent in the fuel. The concentration of nitrogen in the natural gas supplied by the Beijing City natural gas pipeline is 0.52% [18]. Thus, the proportion of NO<sub>x</sub> in the fuel was small, and thermal NO<sub>x</sub> accounts for more than 90% of the total NO<sub>x</sub> emissions [28].

Pourhoseini [29] injected a silver-water nanofluid into a natural gas flame and studied its impact on NO<sub>x</sub> emissions. The mechanism of NO<sub>x</sub> emission reduction by water spraying was clearly explained. The spray water in the combustion air evaporates and absorbs heat during combustion, decreasing the maximum temperature of the flame. Temperature is the

main factor affecting the formation of thermal NO<sub>x</sub>, and after the combustion of air humidification, the maximum flame temperature decreases, and therefore, nitrogen oxide concentration decreases. Dissociation of water can improve the OH radical concentration. OH radicals catalyze the oxidation of CO to consume O atoms. Consequently, the concentration of O atoms in the flame reaction zone decreased, reducing the formation of nitrogen oxides. This is also the reason for the reduction in NO<sub>x</sub> emissions. Pugh et al. [30] confirmed that humidification combustion could reduce NO<sub>x</sub> emissions through these two aspects in experiments using different burners.

### *Relationship between factors that affect NO<sub>x</sub> concentration*

Experimental studies were conducted on variables, such as F<sub>s</sub>, LGR, H<sub>a</sub>, T<sub>a</sub>, operation mode, and T<sub>s</sub>. Fig. 14 shows the relationship analysis of the influencing factors. The flow of spray water affects the LGR of exchanger B and the temperature and humidity of the combustion air. Combustion air humidity affects the concentration of NO<sub>x</sub> in the boiler exhaust gas. Different system operating modes affect the spray water temperature and thus the combustion air temperature. The combustion air temperature affects the humidity and concentration of nitrogen oxides in the boiler exhaust gas. Therefore, the key factor is combustion air humidity.

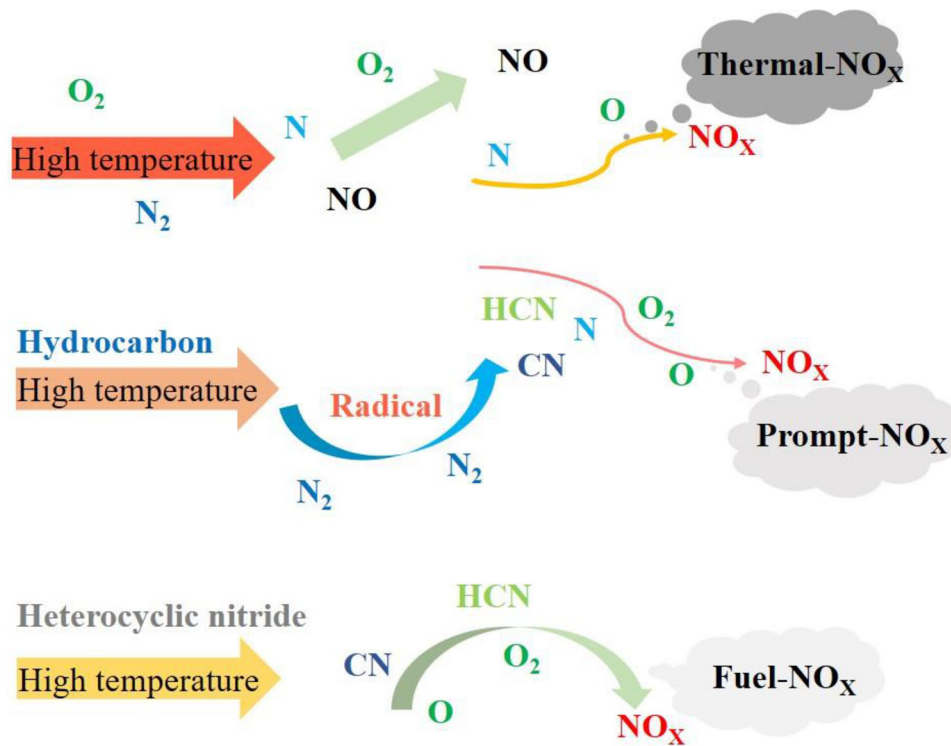


Figure 13. Formation mechanism of NO<sub>x</sub> in gas boiler.

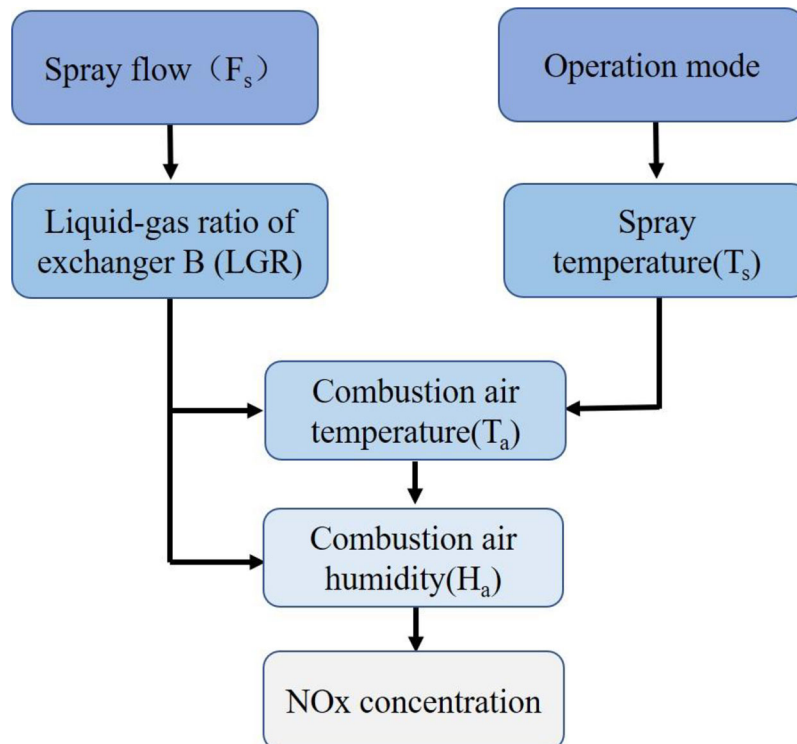


Figure 14. Relationship analysis of influencing factors.

### Economic feasibility analysis

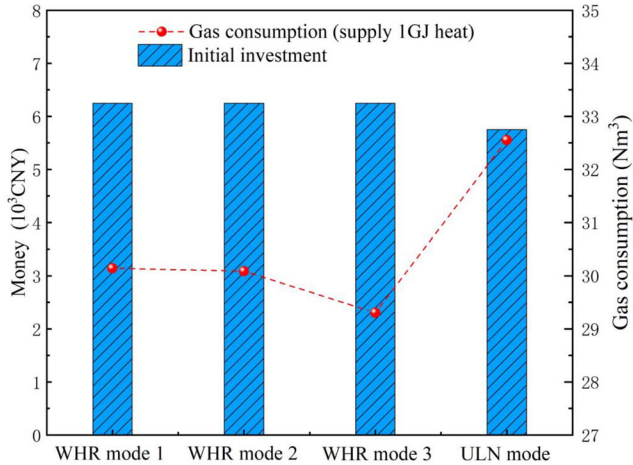
In this section, we compare the economics of the different operating modes in terms of the initial investment and operating costs. The initial investment amounts for

the FGLNHR-CAH system are presented in Table 5. The ULN mode does not have a plate heat exchanger, thus, the initial investment is lower than that of the WHR operating mode, as shown in Fig. 15. The operating costs



**Table 5.** Initial investment of the FGLNHR-CAH system.

Items	Price (CNY)
Spray tower	3100
Water pump	1550
Water pipe, elbow	1000
Plate heat exchanger	500
Flue gas pipeline	60
Spray nozzle	40

**Figure 15.** Comparison of initial investment and gas consumption (maximum air humidity).

of the different modes differ because of their different total efficiencies. The amount of natural gas consumed by each mode to supply 1 GJ of heat was compared under the working conditions with the best NO<sub>x</sub> emission reduction effect, as shown in Fig. 15. It can be observed that the natural gas consumption of the WHR mode is smaller than that of the ULN mode, which can also indicate that the WHR mode has lower operating costs.

$$B = \frac{Q_{out}}{Q_{net,ar} \times \eta_{Total}} \quad (16)$$

where  $B$  is the natural gas consumption, Nm<sup>3</sup>/h,  $Q_{out}$  is the output heat of the gas boiler (kW),  $Q_{net,ar}$  is the low calorific value of natural gas, kJ/Nm<sup>3</sup>, and  $\eta_{Total}$  is the total system efficiency.

Therefore, the ULN mode is suitable for strict NO<sub>x</sub> emission standards, but its operating costs are higher. The WHR mode NO<sub>x</sub> emission reduction effect is not as good as that of the ULN mode, but this mode can recover waste heat and has a better energy-saving effect. It is worth noting that the initial investment of the two modes is low, which has the advantage of a low NO<sub>x</sub> transformation in the gas boiler.

## Conclusions

In this study, a flue gas with low NO<sub>x</sub> emission and WHR system using combustion air humidification technology is proposed (FGLNHR-CAH). The effects

of high air humidity, WHR mode, and other factors on the NO<sub>x</sub> emission reduction and efficiency of the system were studied. The emission reduction mechanism of this technology is also discussed. The technical economies of the two operating modes were evaluated. The primary results of this study are as follows:

1. Combustion air humidification can significantly reduce NO<sub>x</sub> emissions but will affect the boiler efficiency slightly. However, the proposed WHR mode can effectively improve the total efficiency.
2. The ULN mode can obtain higher humidity combustion air, reducing NO<sub>x</sub> emissions to 23.3 mg/m<sup>3</sup>. The boiler efficiency under these conditions was 86.9%.
3. The WHR mode can improve efficiency, but adversely affects the NO<sub>x</sub> emission reduction effect. WHR mode 1 can reduce NO<sub>x</sub> emission to 39.9 mg/m<sup>3</sup> while increasing the total system efficiency to 93.8%.
4. Through an economic analysis, the ULN mode was found to be more suitable for strict emission standards. The WHR mode reduces the NO<sub>x</sub> emission reduction rate; however, this mode can recover waste heat and has a better energy-saving effect. The FGLNHR-CAH system has the advantages of easy implementation, low cost, and good NO<sub>x</sub> emission reduction and promotion.

## Acknowledgements

This work was supported by “The Fundamental Research Funds for Beijing University of Civil Engineering and Architecture” [X20026 \ X20027]; and the BUCEA Post Graduate Innovation Project. Xiaohu Yang greatly acknowledged the support by the K. C. Wong Education Foundation.

## Notes on contributors



**Qunli Zhang** is a full professor in School of Environment and Energy Engineering, Beijing University of Civil Engineering and Architecture, China. He received his Ph.D. in heating ventilation and air conditioning engineering from Tsinghua University in 2007. His research focuses on the waste heat recovery and energy savings in buildings.



**Wenqiang Zhao** is a postgraduate at the School of Environment and Energy Engineering, Beijing University of Civil Engineering and Architecture, China. He obtained his bachelor's degree in heating ventilation and air conditioning engineering from Shanxi University in 2019.



**Donghan Sun** is a postgraduate at the School of Environment and Energy Engineering, Beijing University of Civil Engineering and Architecture, China. He obtained his bachelor's degree in heating ventilation and air conditioning engineering from Beijing University of Civil Engineering and Architecture in 2016.



**Xiangzhao Meng** is a full professor in School of Human Settlements and Civil Engineering, Xi'an Jiaotong University, China. He received his Ph.D. in energy and power engineering from Xi'an Jiaotong University in 2006. His research focuses on the air-conditioning technology and energy savings in buildings.



**Kamel Hooman** is a full professor at Process & Energy Department in Delft University of Technology, The Netherlands. He has served as editor for many prestigious journals including Int. J Heat Mass Transf and Heat Transf Eng. His research focuses on the enhancement of heat transfer in thermal applications, energy savings, thermodynamics, and district heating.



**Xiaohu Yang** is a full professor in School of Human Settlements and Civil Engineering, Xi'an Jiaotong University, China. He received his Ph.D. in energy and power engineering from Xi'an Jiaotong University in 2015. He is the subject editor of Adv. Appl. Energ. His research focuses on the enhancement of heat transfer and energy savings in building.

## ORCID

Xiaohu Yang  <http://orcid.org/0000-0002-1129-6682>

## References

- [1] L. Zhang, et al., "The increasing district heating energy consumption of the building sector in China: Decomposition and decoupling analysis," *J Clean Prod*, vol. 271, pp. 122696, Oct 2020. DOI: [10.1016/j.jclepro.2020.122696](https://doi.org/10.1016/j.jclepro.2020.122696).
- [2] J. Wang, Z. Zhou, J. Zhao, J. Zheng and Z. Guan, "Towards a cleaner domestic heating sector in China: Current situations, implementation strategies, and supporting measures," *Appl Therm Eng*, vol. 152, pp. 515–531, Apr 2019. DOI: [10.1016/j.applthermaleng.2019.02.117](https://doi.org/10.1016/j.applthermaleng.2019.02.117).
- [3] I. A. Shah, et al., "Experimental study on NO<sub>x</sub> emission characteristics of oxy-biomass combustion," *J Clean Prod*, vol. 199, pp. 400–410, Oct 2018. DOI: [10.1016/j.jclepro.2018.07.022](https://doi.org/10.1016/j.jclepro.2018.07.022).
- [4] X. Lu, et al., "Progress of air pollution control in China and its challenges and opportunities in the ecological civilization era," *Engineering*, vol. 6, no. 12, pp. 1423–1431, Dec 2020. DOI: [10.1016/j.eng.2020.03.014](https://doi.org/10.1016/j.eng.2020.03.014).
- [5] J. Wu, Z. Wu, L. Li, Z. Kang and J. Deng, "Numerical simulation of impacts of water injection on performance of natural gas engines," *Journal of Tongji University (Natural Science)*, vol. 47, no. 12, pp. 1809–1816, 2019. (In Chinese).
- [6] M. Jonsson and J. Yan, "Humidified gas turbines—a review of proposed and implemented cycles," *Energy*, vol. 30, no. 7, pp. 1013–1078, Jun 2005. DOI: [10.1016/j.energy.2004.08.005](https://doi.org/10.1016/j.energy.2004.08.005).
- [7] W. Chen, et al., "Experimental study on effects of supply-air humidification on energy and emission performance of domestic gas boilers," *Energy Buildings*, vol. 209, pp. 109726, Feb 2020. DOI: [10.1016/j.enbuild.2019.109726](https://doi.org/10.1016/j.enbuild.2019.109726).
- [8] V. Rajabi and E. Amani, "A computational study of swirl number effects on entropy generation in gas turbine combustors," *Heat Transfer Eng*, vol. 40, no. 3-4, pp. 346–361, 2018. DOI: [10.1080/01457632.2018.1429056](https://doi.org/10.1080/01457632.2018.1429056).
- [9] R. Rabari, S. Mahmud, A. Dutta and M. Biglarbegian, "Effect of convection heat transfer on performance of waste heat thermoelectric generator," *Heat Transfer Eng*, vol. 36, no. 17, pp. 1458–1471, 2015. DOI: [10.1080/01457632.2015.1010925](https://doi.org/10.1080/01457632.2015.1010925).
- [10] H. Jaber, T. Lemenand, M. Ramadan and M. Khaled, "Hybrid heat recovery system applied to exhaust gases—thermal modeling and case study," *Heat Transfer Eng*, vol. 42, no. 2, pp. 106–119, 2019. DOI: [10.1080/01457632.2019.1692495](https://doi.org/10.1080/01457632.2019.1692495).
- [11] J. Yamashita and Y. Utaka, "Improvement in performance of secondary heat exchanger for gas water heater by using narrow tubes," *Heat Transfer Eng*, vol. 36, no. 14-15, pp. 1282–1291, 2014. DOI: [10.1080/01457632.2015.995000](https://doi.org/10.1080/01457632.2015.995000).
- [12] M. Khaled and M. Ramadan, "Study of the thermal behavior of multi tube tank in heat recovery from chimney—analysis and optimization," *Heat Transfer Eng*, vol. 39, no. 5, pp. 399–409, 2017. DOI: [10.1080/01457632.2017.1312864](https://doi.org/10.1080/01457632.2017.1312864).
- [13] X. Zhao, L. Fu, T. Sun, J. Wang and X. Wang, "The recovery of waste heat of flue gas from gas boilers," *Sci Technol Built En*, vol. 23, no. 3, pp. 490–499, May 2017. DOI: [10.1080/23744731.2016.1223976](https://doi.org/10.1080/23744731.2016.1223976).
- [14] J. Hou, D. Che, Y. Liu and Q. Jiang, "A new system of absorption heat pump vs. boiler for recovering heat and water vapor in flue gas," *Energy Procedia*, vol. 152, pp. 1266–1271, Oct 2018. DOI: [10.1016/j.egypro.2018.09.180](https://doi.org/10.1016/j.egypro.2018.09.180).
- [15] C. Lee, B. Yu, D. Kim and S. Jang, "Analysis of the thermodynamic performance of a waste-heat-recovery boiler with additional water spray onto combustion air stream," *Appl. Therm. Eng*, vol. 135, pp. 197–205, May 2018. DOI: [10.1016/j.applthermaleng.2017.11.060](https://doi.org/10.1016/j.applthermaleng.2017.11.060).

- [16] J. Wang, J. Hua, L. Fu and D. Zhou, "Effect of gas nonlinearity on boilers equipped with vapor-pump (BEVP) system for flue-gas heat and moisture recovery," *Energy*, vol. 198, pp. 117375, May 2020. DOI: [10.1016/j.energy.2020.117375](https://doi.org/10.1016/j.energy.2020.117375).
- [17] W. Chen, W. Shi, B. Wang, S. Shang and X. Li, "A deep heat recovery device between flue gas and supply air of gas-fired boiler by using non-contact total heat exchanger," *Energy Procedia*, vol. 105, pp. 4976–4982, May 2017. DOI: [10.1016/j.egypro.2017.03.994](https://doi.org/10.1016/j.egypro.2017.03.994).
- [18] Q. Zhang, et al., "Experimental study of flue gas condensing heat recovery synergized with low NOx emission system," *Appl. Energ.*, vol. 269, pp. 115091, Jul 2020. DOI: [10.1016/j.apenergy.2020.115091](https://doi.org/10.1016/j.apenergy.2020.115091).
- [19] Y. Men, X. Liu, T. Zhang, X. Xu and Y. Jiang, "Novel flue gas waste heat recovery system equipped with enthalpy wheel," *Energ Convers Manage*, vol. 196, pp. 649–663, Sep 2019. DOI: [10.1016/j.enconman.2019.06.026](https://doi.org/10.1016/j.enconman.2019.06.026).
- [20] Y. Fei, *Error Theory and Data Processing*, 7th ed. Beijing, China Machine Press, 2015, (In Chinese)
- [21] Z. Wang, et al., "Study on the formation of NO<sub>2</sub> in gas-fired boiler," *CIESC Journal*, vol. 70, no. 8, pp. 3121–3131, 2019. (In Chinese).
- [22] R. E. Padilla, D. Escofet-Martin, T. Pham, W. J. Pitz and D. Dunn-Rankin, "Structure and behavior of water-laden CH<sub>4</sub>/air counterflow diffusion flames," *Combust Flame*, vol. 196, pp. 439–451, Oct 2018. DOI: [10.1016/j.combustflame.2018.06.037](https://doi.org/10.1016/j.combustflame.2018.06.037).
- [23] M. Michael, S. Howard, B. Daisie and B. Margaret, *Fundamentals of Engineering Thermodynamics*, 7th ed. Massachusetts, USA: John Wiley & Sons, Inc, 2011,
- [24] P. Gray and S. Hawking, "Yakov Borisovich Zel'dovich 1914-1987," *Combust Flame*, vol. 81, pp. 93–95, Aug 1990.
- [25] C. P. Fenimore, "Formation of nitric oxide in pre-mixed hydrocarbon flames," *P Combust Inst*, vol. 13, no. 1, pp. 373–380, 1971. DOI: [10.1016/S0082-0784\(71\)80040-1](https://doi.org/10.1016/S0082-0784(71)80040-1).
- [26] Ø. Skreiberg, P. Kilpinen and P. Glarborg, "Ammonia chemistry below 1400 K under fuel-rich conditions in a flow reactor," *Combust Flame*, vol. 136, no. 4, pp. 501–518, 2004. DOI: [10.1016/j.combustflame.2003.12.008](https://doi.org/10.1016/j.combustflame.2003.12.008).
- [27] C. Lupiáñez, I. Guedea, I. Bolea, L. I. Díez and L. M. Romeo, "Experimental study of SO<sub>2</sub> and NOx emissions in fluidized bed oxy-fuel combustion," *Fuel Process Technol*, vol. 106, pp. 587–594, Feb 2013. DOI: [10.1016/j.fuproc.2012.09.030](https://doi.org/10.1016/j.fuproc.2012.09.030).
- [28] H. Chen, B. Xie, J. Ma and Y. Chen, "NOx emission of biodiesel compared to diesel: Higher or lower?," *Appl Therm Eng*, vol. 137, pp. 584–593, Jun 2018. DOI: [10.1016/j.applthermaleng.2018.04.022](https://doi.org/10.1016/j.applthermaleng.2018.04.022).
- [29] S. H. Pourhoseini, "Enhancement of radiation characteristics and reduction of NOx emission in natural gas flame through silver-water nanofluid injection," *Energy*, vol. 194, pp. 116900, Mar 2020. DOI: [10.1016/j.energy.2020.116900](https://doi.org/10.1016/j.energy.2020.116900).
- [30] D. G. Pugh, et al., "Dissociative influence of H<sub>2</sub>O vapor/spray on lean blowoff and NOx reduction for heavily carbonaceous syngas swirling flames," *Combust Flame*, vol. 177, pp. 37–48, Mar 2017. DOI: [10.1016/j.combustflame.2016.11.010](https://doi.org/10.1016/j.combustflame.2016.11.010).